# Object Space Segmentation by Geometric Reference Structures *

Pankaj K. Agarwal† David Brady‡ Jiří Matoušek§

September 8, 2005

**Abstract**

Segmentation of an object space by binary radiation sensors and geometric reference structures is studied in this paper. Given a family of binary radiation sensors and a geometric reference structure, we refer to the set of sensor states induced by a source at point $p$ as the signature of $p$. We study the segmentation of an object space into signature cells and prove near-optimal bounds on the number of distinct signatures induced by a point source, as a function of sensor and reference structure complexity. We also show that almost any family of signatures can be implemented under this model.

## 1 Introduction

A sensor system implements a mapping between an object state and a sensor state. In the case of radiation field sensors, objects and sensors are embedded in a physical space and the mapping is mediated by field propagation. Conventionally, radiation field sensors have been designed to implement simple isomorphisms of the object state (as in photography) or continuous transformations of the object distribution (as in tomography). With increasingly sophisticated digital processing, however, a wider range of object-sensor mappings have become of interest.

Surprisingly little is known regarding classes of object-sensor mappings implementable on radiation fields. Many studies focus on object-field-sensor mappings as inverse problems, but few have considered the range of implementable mappings. Recently, projects such as DARPA's Integrated

*Research by the first author is supported by NSF under grants CCR-00-86013 EIA-98-70724, EIA-01-31905, and CCR-02-04118, and by a grant from the U.S.–Israel Binational Science Foundation. Applications of this work to biometric sensor networks is supported by Army Research Office grant DAAD19-03-1-0352.

†Department of Computer Science, Box 90129, Duke University, Durham NC 27708-0129; pankaj@cs.duke.edu

‡Department of Electrical and Computer Engineering, Box 90291, Duke University, Durham, NC 27708; dbrady@duke.edu

§Department of Applied Mathematics and Institute for Theoretical Computer Science, Charles University, Malostranské nám. 25, 118 00 Praha 1, Czech Republic; matousek@kam.mff.cuni.cz

Sensing and Processing program have considered joint optimization of inverse problems and mapping design. To pursue such optimization, however, one must have a general grasp on the design space of physically achievable mappings.

This paper considers the potential design complexity of a particularly simple radiation sensor system. We consider strictly geometric field propagation, in which case the object-sensor mapping is determined by the visibility of object points from a particular detector. The visibility is modulated by optical structures placed between detectors and objects. Object estimation under this approach may be termed *reference structure tomography* (RST). RST uses multidimensional optical structures to encode object-sensor mappings [2]. The reference structure is an absorbing, scattering or refracting material that modulates radiation between objects and sensors. Reference structure tomography consists of object analysis based on sensor data and prior knowledge of the reference structure. *Geometric* RST describes reference structure tomography under a geometrical optics model for field propagation. Geometric RST may be regarded as a generalization of coded aperture imaging [4, 6], in which a 2D mask modulates projections from source points onto a detector array and the impulse response is equal to the aperture. Deconvolution of the detected 2D signal on the aperture pattern produces a focused image. RST replaces the coded aperture with a multidimensional pattern and generalizes the logical structure of coded aperture systems to multidimensional segmentation of the object space.

Careful consideration of concepts of space in sensing and sensor networks is fundamental to generalized consideration of object-sensor mappings. Spaces of interest include the physical space through which the radiation propagates as well as subspaces occupied by objects, reference structures and detectors. In addition to these physical spaces we refer to abstract spaces such as the *sensor space* spanned by the sensor states and the *configuration space* spanned by the object states. Previous studies have shown that reference structure tomography enables novel associations between these spaces. For example,

1. The dimensionality of the physical subspace occupied by detectors may be less than the dimesionality of the object space. In conventional fan-beam computed tomography, one reconstructs a 2D source distribution from measurements distributed over 2D space-time (i.e. spatial sampling on a ring surrounding the source over time as the illumination field is restructured.) Using a reference structure, it is possible to directly reconstruct a 3D source from measurements on a 2D boundary without temporal scanning [9].

2. The number of sensor samples may be less than the number of resolution cells in the reconstructed image. Using multiple measurements between the object and the sensors, RST enables compressive transformations between objects and measurements[2].

3. The object-sensor mapping may be considered as a mapping between the object configuration space and the sensor space, rather than a mapping on physical space. The configuration space is not a radiation space. The configuration space for a solid object may consist, for example, of the cross-sectional area of the object. RST can be used to segment and analyze this configuration space without imaging [10].

While RST can redefine and reshape spatial relationships, reference structures cannot implement arbitrary mappings between object and sensor states. The challenge of reference structure

design is to match physically realizable mappings to logically desirable mappings. In this paper we illustrate physical constraints on realizable mappings by bounding the number of *signatures* that can be realized for a particular reference structure geometry.

The sensor system model considered here consists of geometric radiation field propagation and opacity-based field modulation. As illustrated in Fig. 2, under this model the signature field segments the object space into cells with constant signatures. The number, structure, and distribution of these cells is of profound interest to the design and data analysis of a sensor system. Important questions not addressed in this paper include the size and shape distribution of the signature cells, relationships between measures on the sensor space, the object space and the object configuration space. Details of physical realization of this sensor system and approximations necessary to maintain the geometric visibility model are also unaddressed.

Results described herein are also significant in the context of sensor networks and distributed sensor systems. The signature field induced by sensor field of view and sensor distribution critically determines the capacity of sensor systems to track objects. Chakrabarty *et al.* have previously considered signatures and tracking under a particular sensor visibility function [3]. While the radiation and sensing model described here is not completely general, it does illustrate the potential range and subtlety of potential mappings. Similar challenges have been considered in the context of art gallery problems [8]. In conventional art gallery problems sensor nodes are represented as cameras or watchman. The sensor receiver pattern consists of a line through the sensor node. One may consider the sensor model presented here as a generalization on the camera model in art galleries. The addition of more complex radiation and sensing models to art gallery analysis yields new perspectives on both conventional tracking and visibility problems and on novel object analysis and clustering problems. Results presented here, focusing primarily on the coding complexity of the object space-sensor space mapping, provide a hint of the range of new problems.

## 2 Our Model and Results

The context for the work described here includes the rapidly developing field of computational sensing and imaging [7]. As researchers in this field span a wide range from physical optoelectronics to computational geometry, it is important to describe our sensor system model as clearly and broadly as possible. A model for radiation-field sensor system consists of the following:

1. A radiation space. Figure 2 illustrates a radiation space consisting of $\mathbb{R}^2$. Objects, optical elements and field sensors are embedded in the radiation space. The subspace where the point-source object may lie is referred to as the *object space*.

2. A *model* mapping the object state into a field state. Objects generate fields or scatter ambient fields to produce radiation signals. In this paper we limit our attention to point objects.

3. A model for field propagation. Objects induce a local state on the radiation field. The field in the object-containing subspace is transformed by propagation into a field state at points remote from the objects. This paper considers a geometric optics, or *ray-based*, model for field propagation.

4. A model for field modulation by optical elements. Fields are modulated by optical elements that refract, diffract or absorb. This paper considers particularly simple optical elements consisting of absorptive *obscurants* (or *occluders*) that block field propagation.

5. A model for field-sensor state transduction. This paper assumes that sensor points locally sample the field state, e.g., in Figure 2, the field state is sampled at $s_1$ and $s_2$. We assume that the field state is binary, with a value of 1 if any active object point is visible and 0 if no active object point is visible.

While the assumptions made above are not general to all physical systems, they provide the simplest model for analysis and explanation of RST-based spatial segmentation.

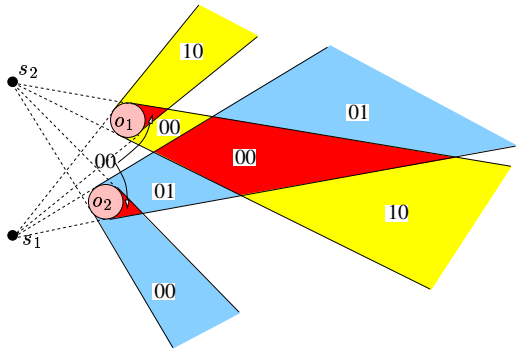


**Figure 1.** A segmentation of the object space by radiation sensors and occluders. $\Pi(\mathcal{S},\ obs) = \{00, 01, 10, 11\}$. The non-shaded area has signature 11, the regions having the same signature may be disconnected.

Let $\mathbb{P} \subseteq \mathbb{R}^d$ denote the radiation space, and let $\mathcal{O} = \{o_1, \ldots, o_n\}$ denote a family of $n$ occluders in $\mathbb{P}$. We assume that each $o_i$ is a convex, semialgebraic set of constant description complexity.[1] Let $\mathbb{X} \subseteq \mathbb{P}$ denote the subspace where sensors are located, and let $\mathcal{S} = \{s_1, \ldots, s_m\}$ be a set of $m$ point sensors located in $\mathbb{X}$. Finally, let $\Sigma$ denote the *object space* where the point source lies. For a point $p \in \Sigma$, a sensor $s_i \in \mathcal{S}$ returns 1 (resp. 0) if $p$ is visible (resp. not visible) from $s_i$, i.e., the segment $s_i p$ does not intersect the interior of any occluder. We use $\chi_i(p)$ to denote the value returned by sensor $s_i$. We define a function $\chi : \Sigma \to \{0,1\}^m$ where $\chi(p) = \chi_1(p) \cdots \chi_m(p)$. We refer to $\chi(p)$ as the *signature* of $p$. Let $\Pi(\mathcal{S}, \mathcal{O}, \Sigma) = \{\chi(p) \mid p \in \Sigma\}$ denote the set of signatures realized by $\mathcal{S}$ and $\mathcal{O}$ in $\Sigma$. Set $\pi(\mathcal{S}, \mathcal{O}, \Sigma) = |\Pi(\mathcal{S}, \mathcal{O}, \Sigma)|$. If $\Sigma = \mathbb{R}^d$, we define

$$\pi_d(m, n) = \max_{\substack{|\mathcal{S}|=m \\ |\mathcal{O}|=n}} \pi(\mathcal{S}, \mathcal{O}, \mathbb{R}^d).$$

The first two results prove bounds on $\pi_d(m, n)$.

**Theorem 2.1** *For any $d \geq 1$ and for any $m, n \geq 1$, $\pi_d(m, n) = O((mn)^d)$.*

[1] A set is *semialgebraic* if it can be expressed as a Boolean combination of polynomial inequalities. A semialgebraic set has *constant description complexity* if it can be defined by polynomials whose number and maximum degree are bounded by some constant.

**Theorem 2.2** *For $m, d \geq 1$ and for any $n$ in range from 1 to $2^m$,*

$$\pi_d(m, n) = \Omega\left(\left(\frac{mn}{\log n}\right)^d\right).$$

Next, we show that one can realize almost any family of signatures even if $\Sigma$ is a line.

**Theorem 2.3** *Let $\mathbb{X}$ be the $x$-axis, and let $\Sigma$ be the line $y = 2$. Given any set $\Pi \subset \{0,1\}^m$, there exists a set $\mathcal{S}$ of $m$ sensors and a set $\mathcal{O}$ of occluders so that $\Pi(\mathcal{S}, \mathcal{O}, \Sigma) = \Pi \cup \{0^m\}$.*

# 3 Upper Bounds

For a pair $s_i \in \mathcal{S}$ and $o_j \in \mathcal{O}$, let $C_{ij}$ denote the cone formed by the set of rays that emanate from $s_i$ and pass through $o_j$. Let $F_{ij}$ be the *frustum* formed by the closure of the portion of $C_{ij}$ that does not lie in the convex hull of $s_i \cup o_j$, i.e.,

$$F_{ij} = \mathrm{cl}(C_{ij} \setminus \mathrm{conv}(s_i \cup o_j)).$$

Note that $\chi_i(p) = 0$, for a point $p \in \Sigma$, if and only if $p \in \bigcup_{i=1}^{n} F_{ij} \cap \Sigma$. Let $\Gamma = \{\gamma_{ij} = F_{ij} \cap \Sigma \mid 1 \leq i \leq m, 1 \leq j \leq n\}$.[2] Since every occluder in $\mathcal{O}$ has constant description complexity, each $\gamma_{ij}$ is a region of constant description complexity.

We define the *arrangement* of $\mathcal{A}(\Gamma)$ to be the decomposition of $\Sigma$ into maximal connected regions, called *cells*, so that all points within the same region lie in the same subset of $\Gamma$. By a well-known result [1], $\mathcal{A}(\Gamma)$ has $O((mn)^d)$ cells. Moreover, for any pair of points $p, q$ lying in the same cell of $\mathcal{A}(\Gamma)$, $\chi(p) = \chi(q)$. Hence, $\pi(\mathcal{S}, \mathcal{O}, \Sigma)$, the number of signatures induced by $\mathcal{S}$ and $\mathcal{O}$ on $\Sigma$ is $O((mn)^d)$. This completes the proof of Theorem 2.1.

Note that many cells of $\mathcal{A}(\Gamma)$ can have the same signature, so it is not obvious that the above bound is tight. In the next section we show that there exists systems of $\mathcal{S}$ and $\mathcal{O}$ for which the above bound is almost tight.

**Remark.** If $\mathbb{P} = \mathbb{R}^2$, then the boundary of $C_{ij}$ consists of two rays, each emanating from $s_i$, so the bound on $\pi_d(m, n)$ does not depend on the complexity of each of occluder and we do not have to assume them to be of constant description complexity. However if $\mathbb{P} = \mathbb{R}^3$, then $\partial C_{ij}$ depends on the complexity $o_j$, and we need the constant-description-complexity assumption.

# 4 Lower Bounds

In this section we prove that Theorem 2.1 is almost tight. We first prove the bound for the case in which $\Sigma$ is a line, and then we cascade multiple copies of this construction to prove lower bounds for $d > 1$.

[2] We are assuming that the object $p$ does not lie inside any occluder, so we do not care about $\chi_i(p)$ for $p \in o_j$.

## 4.1 The $1D$ object space

In our construction, $\mathbb{X}$ is the $x$-axis, $\Sigma$ is the line $y = 2$, and all the occluders, each of which is an interval, are placed on the line $\ell_1 : y = 1$. First we consider the case $n \geq m$. Without loss of generality, we can assume that $m \geq m_0$ for sufficiently large constant $m_0 \geq 1$. We also assume that $n \leq c_0 2^m$ for a suitable constant $c_0 \leq 1$, since we obviously have the lower bound $\pi_1(m, n) = \Omega(m)$ for all $m, n \geq 1$.

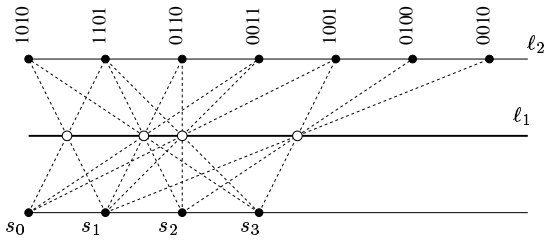


**Figure 2.** 1D lower-bound construction.

We set $\mathcal{S} = \{s_0, \ldots, s_{m-1}\}$, where $s_i = (2i, 0)$. $\mathcal{O}$ is a set of intervals. For simplicity, we describe the construction with degenerate occluders in the sense that $\ell_1 \setminus \bigcup \mathcal{O}$ is a set of points called *pin holes* and denoted by $\mathcal{H}$. We will later modify the construction by replacing each $h_i$ by an interval. The points in $\mathcal{H}$ are chosen as follows. Set $N = mn/c \ln n$ where $c \geq 1$ is a constant whose value will be chosen later. We select each $i \in [1..N]$ with probability $p = n/2N = c \ln(n)/m$. Since $n < c_0 2^m$, $p < 1$ provided $c_0$ is sufficiently small. Let $x_1 < \cdots < x_u$ be the set of selected numbers. Then we set $\mathcal{H} = \{(x_1, 1), \ldots, (x_u, 1)\}$, and we set $o_i = ((x_i, 1), (x_{i+1}, 1))$. We also add two additional occluders $o_0 = ((-\infty, 1), (x_1, 1))$ and $o_u = ((x_u, 1), (\infty, 1))$. Finally, for $j \geq 0$, let $\sigma_j = (2j, 2)$.

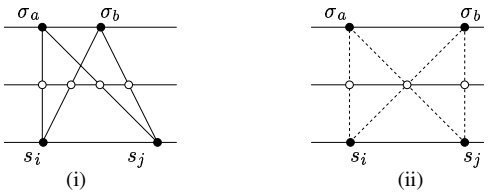


**Figure 3.** (i) A pair of independent integers with respect to $(a, b)$; (ii) $(i, j)$ is not an independent pair with respect to $(a, b)$.

For a pair of indices $0 \leq a \leq b$ and another pair of indices $0 \leq i \leq j \leq m - 1$, we say that the pair $(i, j)$ is *independent with respect to* $(a, b)$ if $\{i + a, j + a\} \cap \{i + b, j + b\} = \emptyset$, which is equivalent to saying that

$$j - i \neq b - a. \tag{1}$$

That is, the intersection points of line $\ell_1$ (which contains $\mathcal{O}$) with the segments $s_i\sigma_a, s_j\sigma_a, s_i\sigma_b$, and $s_j\sigma_b$ are all distinct; Figure 3.

**Lemma 4.1** *For any $0 \leq a \leq b < N - m$, there exists a subset $\mathcal{I} \subseteq [0..m-1]$ of size at least $m/2$ so that every pair of indices in $\mathcal{I}$ is independent with respect to the pair $(a, b)$.*

**Proof:** By (1), for a fixed pair $(a, b)$, each integer $0 \leq i < m$ depends (with respect to $(a, b)$) only on one integer larger than $i$, namely $i + (b - a)$. Therefore we choose

$$\mathcal{I} = \{2i(b-a) + r \mid 0 \leq i \leq \lfloor m/2(b-a) \rfloor, 0 \leq r < b - a\}.$$

By construction, $|\mathcal{I}| \geq m/2$. Moreover, if $k = 2i(b-a) + r \in \mathcal{I}$, then $k + (b-a) = (2i+1)(b-a) + r \notin \mathcal{I}$. Hence, every pair of integers in $\mathcal{I}$ is independent with respect to the pair $(a, b)$. □

**Lemma 4.2** *For $0 \leq a < b < N - m$,*

$$\Pr[\chi(\sigma_a) = \chi(\sigma_b)] \leq \frac{1}{2N^2}.$$

**Proof:** Let $\mathcal{I} \subseteq [0..m-1]$ be a subset of pairwise independent indices (with respect to the pair $(a, b)$) of size at least $m/2$ (Lemma 4.1). Then

$$\begin{aligned}
\Pr[\chi(\sigma_a) = \chi(\sigma_b)] &= \Pr\left[\bigcap_{j=1}^{m} \chi_j(\sigma_a) = \chi_j(\sigma_b)\right] \\
&\leq \Pr\left[\bigcap_{j \in \mathcal{I}} \chi_j(\sigma_a) = \chi_j(\sigma_b)\right] \\
&= \prod_{j \in \mathcal{I}} \Pr\left[\chi_j(\sigma_a) = \chi_j(\sigma_b)\right].
\end{aligned}$$

The last equality follows from the fact that every pair of indices in $\mathcal{I}$ is independent with respect to the pair $(a, b)$, thereby implying that the values of $\chi_i(\sigma_a), \chi_i(\sigma_b), \chi_j(\sigma_a), \chi_j(\sigma_b)$ are all independent. Hence,

$$\Pr[\chi_j(\sigma_a) = \chi_j(\sigma_b)] = p^2 + (1-p)^2 = 1 - 2p(1-p) \leq 1 - p$$

because $p \leq 1/2$. Therefore,

$$\begin{aligned}
\Pr[\chi(\sigma_a) = \chi(\sigma_b)] &\leq (1-p)^{m/2} \leq \exp\left(\frac{-pm}{2}\right) \\
&\leq \exp\left(\frac{-c \ln n}{2}\right) < \frac{1}{N^{c/2}} \leq \frac{1}{2N^2},
\end{aligned}$$

provided $c \geq 10$. This completes the proof of the lemma. □

The above lemma implies that

$$\Pr[\exists a \neq b \; \chi(\sigma_a) = \chi(\sigma_b)] \leq \sum_{0 \leq i < j \leq N} \Pr[\chi(\sigma_a) = \chi(\sigma_b)] \leq \frac{1}{4}.$$

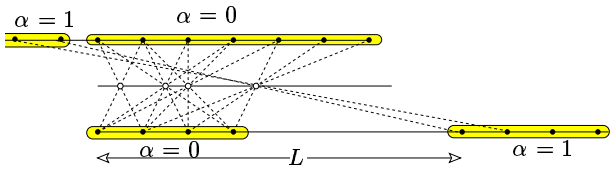


**Figure 4.** Handling small values of $n$.

Since $\Pr[|H| > n] < 1/4$, the probability of $|\mathcal{H}| \leq n$ and $\chi(\sigma_i) \neq \chi(\sigma_j)$, for all $0 \leq i < j \leq N$, is at least $1/4$. Hence, there exists a set $\mathcal{O}$ of $n + 2 \geq m$ occluders so that $\pi(\mathcal{S}, \mathcal{O}, \ell_2) = \Omega(mn/\log(n))$.

Next, we extend the proof to the case $n < m$. For simplicity, we assume that $m$ is divisible by $n$. we construct $\mathcal{O} = \{o_1, \ldots, o_n\}$ as above with $m = n$ so that $\sigma_0, \ldots, \sigma_u$, $u = \Omega(n^2/\log(n))$ have distinct signatures. Let $\chi(\sigma_i) = \omega_i$. We choose a sufficiently large even integer $L \gg n^2$ so that the intersection point of $\ell_2$ with the line passing through $(L, 0)$ and the left endpoint of $o_n$ lies to the left of $\sigma_0$. We set $\mathcal{S} = \{(\alpha L + 2i, 0) \mid 0 \leq i \leq n-1, 0 \leq \alpha < m/n\}$, i.e., we make $m/n$ copies of $n$ sensors, separated by a large interval $L$. We now consider the points $\sigma_{-\alpha L + a}$, for $0 \leq a \leq u$ and $0 \leq \alpha \leq m/n$. We divide a signature into $m/n$ blocks. The bits in the $\alpha$th block of $\chi(\sigma_{-\alpha L+a})$ are the same as that of $\omega_a$ and the remaining bits are $0$. Hence, we get $\Omega(mn/\log(n))$ distinct signatures.

We have thus proved the following:

**Lemma 4.3** *Let $m, n \geq 1$ so that $n \leq 2^m/c_0$, for a constant $c_0$. Set $\mathcal{S} = \{(2i, 0) \mid 0 \leq i < m\}$ and $\sigma_i = (2i, 2)$. There exists a set $\mathcal{O}$ of $n$ occluders on the line $y = 1$ so that for $0 \leq i < j \leq cmn/\log(n)$, $\chi(\sigma_i) \neq \chi(\sigma_j)$, where $c > 0$ is a constant.*

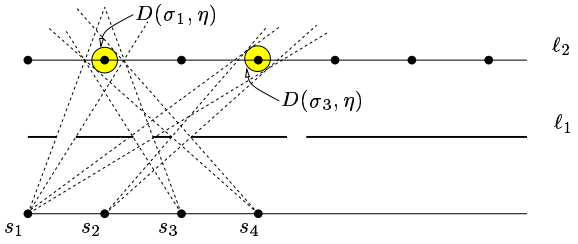


**Figure 5.** Shrinking each occluder $o_i$ by $\delta$. All points in $D(\sigma_1, \eta)$ have the same signature as $\sigma_1$.

It can be shown that even if we replace each point $(x_i, 1) \in \mathcal{H}$ by an interval $[(x_i - \delta, 1), (x_i + \delta, 1)]$, for some $\delta < 1/10$ (i.e., $o_i$ now becomes $[(x_i + \delta, 1), (x_{i+1} - \delta, 1)]$, $\chi(\sigma_a)$ does not change. In fact, there exists a real value $\eta = \eta(\delta) > 0$ so that for all points $p \in D(\sigma_i, \eta)$, the disk of radius $\eta$ centered at $\sigma_i$, $\chi(p) = \chi(\sigma_i)$; see Figure 5. Hence, we can shrink each $o_i$ by $\delta$ at both of its endpoints without changing $\Pi(\mathcal{S}, \mathcal{O}, \ell_2)$.

Putting everything together, we obtain the following.

**Lemma 4.4** *Let $m, n \geq 1$ so that $n \leq 2^m/c_0$, for a constant $c_0$. Set $\mathcal{S} = \{(2i, 0) \mid 0 \leq i < m\}$ and $\sigma_i = (2i, 2)$. There exists a set $\mathcal{O}$ of $n$ occluders on the line $y = 1$, each an interval, and a real value $\eta > 0$ so that for $0 \leq i < j \leq u = \Omega(mn/\log(n))$, (i) $\chi(\sigma_i) \neq \chi(\sigma_j)$ and (ii) all points in $D(\sigma_i, \eta)$ have the same signature.*

## 4.2 Higher dimensional sensor space

We now show how to extend the 1D construction in Lemma 4.4 to 2D to obtain $\Omega((mn/\log(mn))^2)$ distinct signatures. The same approach will extend to $d > 2$ as well.

Let $\mathcal{S}, \mathcal{O}, \eta$, and $u$ be the same as in Lemma 4.4. Let $\omega_i = \chi(\sigma_i)$. Then $\omega_i \neq \omega_j$, for all $1 \leq i \neq j \leq u$, and $\chi(p) = \chi(\sigma_i)$ for all points $p \in D(\sigma_i, \eta)$. Let $R$ be the smallest axis-parallel rectangle that contains $D(\sigma_0, \eta), \ldots, D(\sigma_u, \eta)$. Let $L$ be the length of $R$, and let $\tau$ be the geometric transform (translation in $y$-direction followed by scaling in $y$-direction) that maps $R$ to the square $[0, L]^2$. Let $\mathcal{S}' = \{\tau(s_i) \mid 0 \leq i < m\}$ and $\mathcal{O}' = \{\tau(o_j) \mid 1 \leq j \leq n\}$ be the sets of sensors and occluders in the transformed space, and let $E'_i = \tau(D(\sigma_i, \eta))$; $E_i$ is an ellipse. See Figure 6.

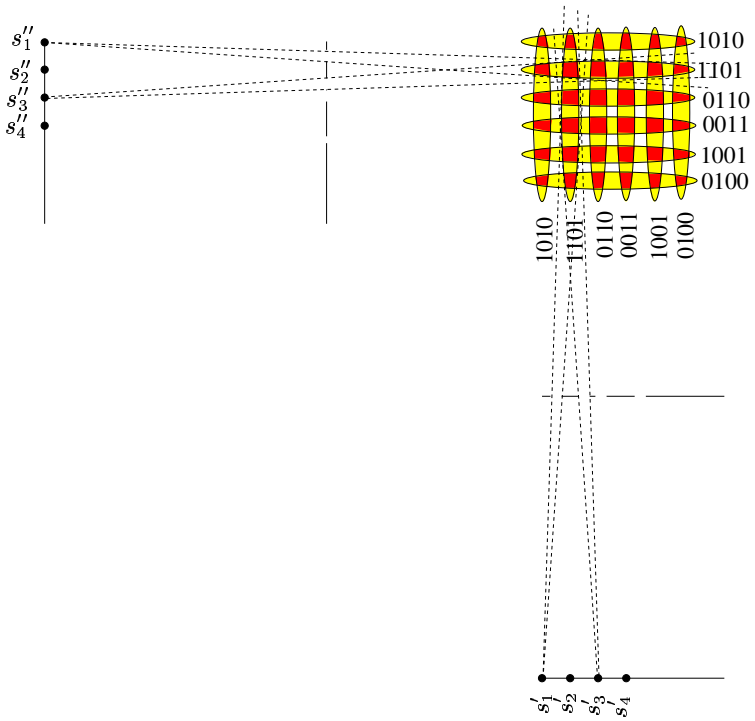


**Figure 6.** Lower-bound construction in 2D.

Next, let $\varrho$ be the reflection transform with respect to the line $y = x$, i.e., $\varrho$ maps a point $(a, b)$ to the point $(b, a)$. Set $\mathcal{S}'' = \varrho(\mathcal{S}')$, $\mathcal{O}'' = \varrho(\mathcal{O}')$, and $E''_i = \varrho(E'_i)$. Finally, let $\mathcal{S} = \mathcal{S}' \cup \mathcal{S}''$ and $\mathcal{O} = \mathcal{O}' \cup \mathcal{O}''$. By construction, for any point $\xi_{ij} \in E'_i \cap E''_j$, $\chi(\xi_{ij}) = \omega_i \circ \omega_j$, the concatenation of

$\omega_i$ and $\omega_j$. Since $\omega_i \neq \omega_j$ for $i \neq j$, $\chi(\xi_{ij})$ is distinct for all pairs $1 \leq i, j \leq u$. Consequently,

$$\pi(\mathcal{S}, \mathcal{O}, \mathbb{R}^2) \geq u^2 = \Omega\left(\frac{m^2 n^2}{\log^2 mn}\right),$$

thereby proving Theorem 2.2 for $d = 2$. The bound for $d > 2$ can be proved in a similar manner.

# 5 Realizing a Family of Signatures

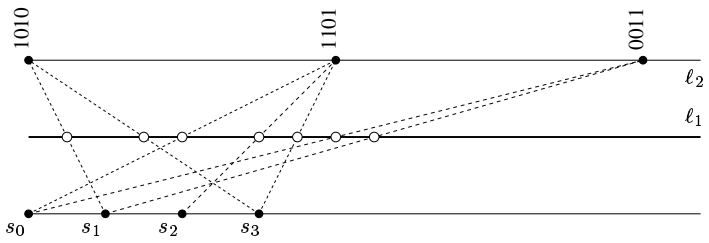


**Figure 7.** Realizing a family of signatures.

We now prove Theorem 2.3. Let $\Pi = \{\pi_0, \ldots, \pi_{N-1}\}$ be a set of signatures, where $\pi_i \in \{0,1\}^m$. We place a family $\mathcal{S} = \{s_0, \ldots, s_{m-1}\}$ of $m$ sensors on the $x$-axis, where $s_i = (2i, 0)$. The object space is the line $\ell_2 : x = 2$. For $0 \leq j \leq N-1$, let $\sigma_j = (2j, 2)$. We will place a set of occulders on the line $\ell_1 : y = 1$ so that $\chi(\sigma_j) = \pi_j$ for $0 \leq j < N$. As in the previous section, we construc degenerate occluders so that $\ell_1 \setminus \bigcup \mathcal{O}$ is a set $\mathcal{H} = \{h_0, \ldots, h_{n-1}\}$ of points. We partition $\mathcal{H}$ into $N$ blocks $\mathcal{H}_0, \ldots, H_{N-1}$, where $\mathcal{H}_j \subset [jm..(j+1)m-1]$. We add the point $(jm+i, 1) \in \mathcal{H}_j$ if $\chi_i(\sigma_j) = 1$, so that $\sigma_j$ is visible from $s_i$. By construction $s_i$ is visible at $\sigma_j$ if and only if $(jm+i, 1) \in \mathcal{H}_j$. Hence, $\chi(\sigma_j) = \pi_j$. For any point $p \in \ell_2 \setminus \bigcup \sigma_j$, $\chi(p) = 0^m$. This completes the proof of Theorem 2.3.

# 6 Conclusions

We have developed formal limits on the complexity of signature fields induced by reference structures and binary sensors. While our methods do not yield optimal reference structure designs, they do constrain the nature of the object-sensor mapping. Optimal design would consider many features not included in this study, such as the topology of the signature field. The possibility of identical or nearly identical signatures for wildly different source states is particularly interesting. Such ambiguities are certain for small sensor and reference structure systems, their probability for complex systems is unexplored.

Relationships between measures on the sensor space and measures on the object space are also of substantial interest. Intuitively, one would like signatures for similar source object states to be similar. The extent to which this is the case in the system described here has yet to be fully explored.

Visibility-based sensor systems based on the model described here are under development at Duke for human biometric and tracking systems. These systems use differential pyroelectric sensor networks as described in [5]. Current versions use lenslet arrays to shape the sensor visibility rather than obscurants and use differential sensor pairs rather than staring sensors. Despite these differences, the conceptual framework laid in this paper for analysis of signature fields is useful in system design. We look forward to continued development of this framework and closer integration of physical design contraints with mathematical limits in future publications.

# References


[1] P. K. Agarwal and M. Sharir, Arrangements and their applications, in: *Handbook of Computational Geometry* (J.-R. Sack and J. Urrutia, eds.), Elsevier Science Publishers B.V. North-Holland, Amsterdam, 2000, pp. 49–119.

[2] D. J. Brady, N. P. Pitsianis, and X. Sun, Reference structure tomography, *Journal of the Optical Society of America A*, 21 (2004), 1140–1147.

[3] K. Chakrabarty, S. S. Iyengar, H. R. Qi, and E. C. Cho, Grid coverage for surveillance and target location in distributed sensor networks, *Ieee Transactions on Computers*, 51 (2002), 1448–1453.

[4] E. E. Fenimore, Coded aperture imaging - predicted performance of uniformly redundant arrays, *Applied Optics*, 17 (1978), 3562–3570.

[5] U. Gopinathan, D. J. Brady, and N. P. Pitsianis, Coded apertures for efficient pyroelectric motion tracking, *Optics Express*, 11 (2003), 2142–2152.

[6] S. R. Gottesman and E. E. Fenimore, New family of binary arrays for coded aperture imaging, *Applied Optics*, 28 (1989), 4344–4352.

[7] J. N. Mait, R. Athale, and J. van der Gracht, Evolutionary paths in imaging and recent trends, *Optics Express*, 11 (2003), 2093–2101.

[8] J. O'Rourke, *Art gallery theorems and algorithms*, Oxford University Press, New York, 1987.

[9] P. Potuluri, M. B. Xu, and D. J. Brady, Imaging with random 3d reference structures, *Optics Express*, 11 (2003), 2134–2141.

[10] A. Sinha and D. J. Brady, Size and shape recognition using measurement statistics and random 3d reference structures, *Optics Express*, 11 (2003), 2606–2618.